



## *Colletotrichum* sp.- mediated synthesis of sulphur and aluminium oxide nanoparticles and its *in vitro* activity against selected food-borne pathogens.



Pooja Suryavanshi<sup>a</sup>, Raksha Pandit<sup>a</sup>, Aniket Gade<sup>a</sup>, Marcos Derita<sup>b</sup>, Susana Zachino<sup>b</sup>, Mahendra Rai<sup>a,\*</sup>

<sup>a</sup> NanobioTech Lab, Department of Biotechnology, SGB Amravati University, Amravati, 444 602, Maharashtra India

<sup>b</sup> Pharmacognosy Area, Faculty of Biochemical and Pharmaceutical Sciences, Suipacha 531, National University of Rosario, Rosario, 2000, Argentina

### ARTICLE INFO

#### Article history:

Received 7 October 2016

Received in revised form

17 March 2017

Accepted 21 March 2017

Available online 23 March 2017

#### Keywords:

Antimicrobial

Essential oils

Mycosynthesis

Nanofunctionalized oils

Nanoparticles

Pathogens

### ABSTRACT

Food spoilage is a major issue globally and million of people suffer from food-borne infections. Hence, there is a need to search for novel and effective antimicrobial agents. Nanoparticles act as antimicrobial agent, which can tackle the problem of food-borne pathogens. The present study includes mycosynthesis of sulphur nanoparticles (SNPs) and aluminium oxide nanoparticles (AINPs) from *Colletotrichum* sp. and their characterization by UV-Vis spectroscopy, Nanoparticles Tracking and Analysis, Zeta potential measurement, X-ray diffraction and Transmission Electron Microscopy. Essential oils (EOs) were extracted from the leaves of *Eucalyptus globulus* and *Citrus medica*. Nanofunctionalized oils were formulated by combining nanoparticles with EOs. *In vitro* antimicrobial activity of SNPs, AINPs, EOs and nanofunctionalized oils was evaluated against selected food-borne pathogens such as *Listeria monocytogenes*, *Salmonella typhi*, *Chromobacterium violaceum*, *Fusarium oxysporum* and *Aspergillus flavus*. The antimicrobial activity of SNPs was found to be maximum against *Salmonella typhi* (21 mm), whereas AINPs were highly effective against *F. oxysporum* (22 mm). It was found that activity of antibiotics such as tetracycline, oxytetracycline, gentamicin, fluconazole, ketoconazole, amphotericin B and nystatin. increase in combination with nanoparticles. Nanofunctionalized oil can be used as a novel antimicrobial agent the prevention of food spoilage caused by food-borne pathogens.

© 2017 Elsevier Ltd. All rights reserved.

## 1. Introduction

The consumption of food contaminated with pathogenic bacteria and/or their toxins is a widespread health problem, being the major cause of food-borne diseases, such as campylobacteriosis, listeriosis, hemorrhagic colitis and salmonellosis (Käferstein, Mortarjemi, & Bettcher, 1997). Mead et al. (1999) estimated that food-borne agents annually affect 76- million people resulting into 5000 deaths in the United States. In fact, the identification and evaluation of new antimicrobial agents for the control of food-borne pathogens is a global challenge. Nanotechnology has potential for solving the problem of food-borne pathogens. Nanoparticles act as antimicrobial agent due to their small size and high surface/volume ratio, which allows them to interact with target

bacteria (Le et al., 2011; Singh and Singh, 2011). Rai, Yadav, Bridge, and Gade (2009) coined the term “Myconanotechnology” [“Myco” meaning fungi and “nanotechnology” is the manipulation of materials with atleast one dimension in the range of 1–100 nm]. Filamentous fungi have the capacity to secrete proteins, produce large amount of extracellular enzymes, which help in better reduction of precursor material into nanosize material (Saxena, Sharma, Gupta, & Singh, 2014). Moghaddam, Namvar, Moniri, Paridah, and Mohamad (2015) reported that biologically synthesized nanoparticles possess high level of consistency. The knowledge about the mechanistic aspect has helped to control the morphology and size of the nanoparticles during the synthesis process (Yadav et al., 2015). Nanoparticles synthesized from *Colletotrichum* sp. were found to be very stable (ShivShankar, Ahmad, Pasricha, & Sastry, 2003; Rai, Yadav, & Gade, 2011).

Essential oils (EOs) are oily aromatic compound extracted from plants. They are considered as natural antimicrobial agent from ancient era (Mith et al., 2014). EOs are composed of terpenoids such

\* Corresponding author.

E-mail addresses: [pmkrai@hotmail.com](mailto:pmkrai@hotmail.com), [mahendrarai7@gmail.com](mailto:mahendrarai7@gmail.com) (M. Rai).

as monoterpenes, sesquiterpenes, diterpenes and various molecules including acids, alcohols, aldehydes, aliphatic hydrocarbons, lactones, coumarins and homologs of phenyl propanoids (Nazzaro, Fratianni, Martino, Coppola, & Feo, 2013). EOs are hydrophobic and lipophilic in nature due to these attributes, EOs can pass through cell, cytoplasmic membrane, disrupts cell membrane mechanisms and can disturb different layers of polysaccharides, fatty acids, phospholipid content (Ramos et al., 2014). EOs can change the fluidity of cell membrane, which lead to membrane permeability and result into the leakage of ions and proteins. The permeabilization of outer and inner mitochondrial membrane leads to cell death (Faleiro, 2011; Ramos et al., 2014). EOs are volatile in nature and can decompose or evaporate at the time of food processing, preparation of antimicrobial film and formulation of drugs. To improve the stability of EOs at the time of processing and storage, nano-encapsulation of EOs has been applied in food and nutraceutical industries. Encapsulation of EOs can preserve and protect their functional properties, additionally, encapsulation increases antimicrobial activity of EOs (Hyldgaard, Mygind & Mygind, 2012; Hosseini, Zandi, Rezaei, & Farahmandghav, 2013). Encapsulation of EOs in biodegradable nanoparticles like chitosan can be used in food preservation (Hyldgarrd et al., 2012; Pecarsaki, Jugovic, Brankovic, Mihajilovski, & Jankovic, 2014).

In the present study, we report the mycosynthesis of SNPs and AINPs from *Colletotrichum* sp. and evaluated antimicrobial activity of nanoparticles, EOs extracted from *Citrus medica* and *Eucalyptus globulus* and nanofunctionalized EOs (in combination with essential oils and nanoparticles) against selected food-borne *C. violaceum*, *L. monocytogenes*, *S. typhi*, *F. oxysporum* and *A. flavus*. The activity of SNPs and AINPs was also evaluated in combination with tetracycline, oxytetracycline, gentamicin, fluconazole, ketoconazole, amphoterecin B and nystatin.

## 2. Materials and methods

### 2.1. Procurement of materials

Aluminium chloride, sodium thiosulphate, Muller-Hinton broth and agar, Brain Heart Infusion broth and agar, Potato Dextrose broth and agar, potassium bromide powder were purchased from Hi-media PVT Ltd. Mumbai, India.

#### 2.1.1. Preparation of fungal extract and synthesis of nanoparticles

*Colletotrichum* sp. (DBT 349) was procured from Department of Biotechnology, SGB Amravati University, Amravati, India. For the synthesis of nanoparticles, the fungus was inoculated in 100 mL Potato Dextrose Broth (PDB), and incubated for 7 d at 27 °C. Mycelia were harvested by filtering through Whatman's filter paper No 42 and rinsed thrice with sterile double distilled water. Later, mycelia were re-suspended in 100 mL sterile double distilled water and incubated at room temperature for 24 h. It was then passed through membrane filtration assembly. For synthesis of SNPs method described by Awwad, Salem, and Amany (2015) was modified and procedure of Ansari et al. (2015) was modified for the synthesis of AINPs. For synthesis of SNPs, fungal filtrate was treated with 20 mM sodium thiosulphate ( $\text{Na}_2\text{S}_2\text{O}_3$ ), and kept on magnetic stirrer for proper mixing, 1000  $\mu\text{l}$  of concentrated hydrochloric acid was added in drop wise manner. The suspended SNPs were centrifuged at 10,000 g for 20 min, washed thrice with distilled water, dried in oven and further used for characterization. For the synthesis of AINPs, aluminium chloride was used as a precursor salt. The fungal filtrate was treated with 50 mM aluminium chloride ( $\text{AlCl}_3$ ), heated in microwave oven at 640 W for 10 min. After nanoparticle synthesis precipitate was obtained at the bottom of the flask.

### 2.2. Detection and characterization of nanoparticles

#### 2.2.1. Visual observation

The detection of synthesized nanoparticles was primarily carried out by visual observation. After the treatment of fungal filtrate with 20 mM  $\text{Na}_2\text{S}_2\text{O}_3$  yellow turbid solution was formed, which indicates the formation of SNPs whereas, in case of AINPs, brown precipitate was obtained at the bottom of the flask, which showed the formation of AINPs.

#### 2.2.2. UV-Vis spectrophotometer analysis

The preliminary detection of SNPs and AINPs was made by using UV-Visible spectrophotometer (Shimadzu UV-1700, Japan). The aliquots of the synthesized nanoparticles were subjected to UV-Visible analysis by scanning the absorbance spectra from 200 to 800 nm.

#### 2.2.3. Nanoparticle Tracking and Analysis (NTA)

Nanoparticle Tracking and Analysis is a laser-based light scattering system used for determining the size, particle size distribution and concentration of nanoparticles. Analysis was performed by NanoSight LM 20 using a beta version of the NTA 2.3 software (Nanosight Pvt. Ltd., UK). For sample preparation, 7  $\mu\text{l}$  solution of SNPs and AINPs were diluted in 2 mL of nuclease free water.

#### 2.2.4. Zeta potential analysis

Zeta potential is a measure of charge and stability of nanoparticles at pH 7, which was measured by using Zeta sizer (Malvern Zetasizer NanoZS90, UK). For sample preparation, 30  $\mu\text{l}$  of synthesized nanoparticles solution was diluted in 2 mL of nuclease free water. For zeta potential measurement, 1000  $\mu\text{l}$  of the sample was taken in zeta dip cell and placed in Zeta sizer for analysis.

#### 2.2.5. X-ray diffraction (XRD)

X-ray diffraction (XRD) analysis was performed using Rigaku Miniflex II desktop X-ray diffractometer. For the sample analysis, powder samples of SNPs and AINPs were mounted on sample holder ring. After analysis of the samples, Bragg's reflection pattern was obtained and compared with the standard reference file known as File Joint Committee on Powder Diffraction (JCPDS).

#### 2.2.6. Transmission Electron Microscopy (TEM)

TEM (Philips model CM 12) analysis was carried out on carbon-coated copper grid. 5  $\mu\text{l}$  of SNPs and AINPs were placed on copper grids, and allowed to dry in infrared light for 30 min. Size and morphology of nanoparticles were determined by TEM analysis.

### 2.3. Extraction of essential oils (EOs)

EOs were extracted from the leaves of *Eucalyptus globulus* and *Citrus medica* by Clevenger apparatus (Souza et al., 2014).

### 2.4. Formulation of nanofunctionalized oils

Stock solution of (1mg/mL) nanoparticles was taken in deionized water as described by Ahmed, Hiremath, and Jacob (2016), and sonicated. Nanoparticles were mixed with 1 mL of EO. 10  $\mu\text{l}$  of tween-80 was added to it; vortexed for 4 min, and sonicated for 30 min to prevent aggregation and deposition of nanoparticles.

### 2.5. Assessment of antimicrobial activity

#### 2.5.1. Test bacteria

The pure cultures of the food-borne *Listeria monocytogenes* (MTCC 1143), and *Fusarium moniliforme* (MTCC 6636) were

procured from the Microbial Type Culture Collection (MTCC), Chandigarh, India. *Chromobacterium violaceum* (MCC 2290) was obtained from Microbial Culture Collection, Pune, India. *Salmonella typhi* (ATCC 51812) was procured from American Type Culture Collection, Manassas, VA, USA. *Aspergillus flavus* was isolated from peanut (DBT4).

### 2.5.2. In vitro evaluation of antimicrobial activity by disc diffusion method

Synthesized SNPs and AINPs were evaluated against *S. typhi* (ATCC 51812), *C. violaceum* (MTCC 2290), and *L. monocytogenes* (MTCC 1143) by Kirby-Bauer disc diffusion method (Bauer, Roberts, & Kirby, 1960). The antibacterial activity was evaluated against *S. typhi*, *C. violaceum* on Muller Hinton agar plates and *L. monocytogenes* on Brain Heart Infusion agar plates. *S. typhi*, and *C. violaceum* were inoculated into Muller Hinton Broth and incubated at 37 °C for 24 h. *L. monocytogenes* was incubated for 24 h at 37 °C. 100 µl of inoculum (approximate concentration 10<sup>5</sup> CFU/mL) was streaked on the respective agar plates. To determine the activity of SNPs, AINPs, EOs, and nanofunctionalized oils, standard sterile paper discs were impregnated with 20 µl of the above solution, placed them on the surface of agar plates and incubated at 37 °C. The antimicrobial activity of synthesized nanoparticles was also tested in combination with antibiotics, viz., tetracycline, oxytetracycline and gentamicin. The zones of inhibition were recorded in mm and the above assay was performed in triplicate.

For evaluation of antifungal activity of nanoparticles against *A. flavus* and *F. oxysporum*, potato dextrose agar was used. Seven-days old fungal biomass was suspended in RPMI 1640 and its Colony Forming Unit (CFU) was maintained around 0.4 × 10<sup>4</sup> CFU/mL (CLSI, 2002). The 20 µl spore suspension was streaked onto the surface of agar plates. The discs were placed onto the agar surface and incubated at 28 °C for 48 h, followed by the measurement of zones of inhibition. The antifungal activity of synthesized nanoparticles was tested in combination with commercially available antibiotics, such as fluconazole, ketoconazole, amphotericin B and nystatin. The assay was performed in triplicate.

### 2.6. Assessment of increased in fold area

Increase in fold area of commercially available antibiotics, viz. tetracycline, oxytetracycline, gentamicin, fluconazole, ketoconazole, amphotericin B and nystatin was assessed in combination with nanoparticles. Moreover, increase in fold area of nanofunctionalized oils was calculated by using formula (B<sup>2</sup>-A<sup>2</sup>)/A<sup>2</sup> where 'A' is radius of zone of inhibitions formed by antibiotics and EOs, and 'B' is the radius of zones of inhibition of Antibiotics + NPs, and EOs + NPs (Bawaskar et al., 2010).

### 2.7. Evaluation of minimum inhibitory concentration (MIC)

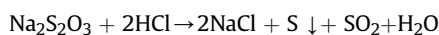
MIC of SNPs and AINPs was determined by microbroth dilution method. For calculating MIC value, the concentration range of nanoparticles was taken from 50 to 1000 µg/µl. To determine MIC of bacteria, Muller-Hinton broth was used for *S. typhi* and *C. violaceum* and Brain Heart Infusion broth for *L. monocytogenes*. The 180 µl of Muller-Hinton broth and Brain Heart Infusion broth was added in each well of 96-well plates. Further, 20 µl of each bacterial culture was added into same well followed by addition of 20 µl nanoparticle solution. The plates were incubated for 24 h at 37 °C. MIC values were recorded after addition of 40 µl of triphenyl tetrazolium chloride (TTC) (0.2 mg/mL) in each well.

To determine MIC of nanoparticles against *A. flavus* and *F. oxysporum*, microbroth dilution method was used in microtitre plate. Fungi were inoculated in RPMI medium and incubated for

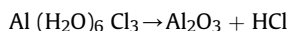
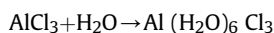
7 d at 25 ± 2° C. The absorbance was measured by using a colorimeter at 530 nm and the fungal load was maintained at 0.4 × 10<sup>4</sup> to 5 × 10<sup>4</sup> CFU/mL. The optical density of the fungal suspension was adjusted between 0.15 and 0.17 by using RPMI medium. This suspension was used for evaluation of activity of nanoparticles. Moreover, 10–80 µg/mL range was taken for calculating MIC value of nanoparticles (Wayne, 2002).

## 3. Results and discussion

The mycosynthesized sulphur and aluminium oxide nanoparticles demonstrated visual colour change. The colourless solution of fungal filtrate changed to yellowish turbid after the synthesis of SNPs. This study showed resemblance with the results obtained by Awwad et al. (2015), who synthesized SNPs by the fruit extract of *Albizia julibrissin*. When sodium thiosulphate solution was treated with hydrochloric acid, disproportionation reaction occurred in the reaction mixture as a result, SNPs were precipitated and sulfonic acid was formed (Awwad et al., 2015).



For AINPs, colourless fungal extract produced brown precipitate. Aluminium chloride is hygroscopic in nature and when it was reacted with filtrate, chloride ions are displaced by water and aluminium hydroxide was formed. After placing in microwave oven, aluminium oxide nanoparticles were produced. The present study showed similarity with the report of Ansari et al. (2015) who reported the formation of brownish-yellow precipitate after the synthesis of aluminium oxide nanoparticles.



UV-Vis spectroscopy is an optical analysis method used for preliminary detection of the SNPs and AINPs. Mycosynthesized SNPs showed maximum absorbance peak at 291 nm, (Fig. 1(A)) which was in agreement with results obtained by Chaudhuri and Paria (2011) who reported that SNPs showed maximum absorbance around 280–300 nm. The absorbance peak of AINPs was noted at 281 nm (Fig. 1(B)) which corroborates the result reported by Sutradhar, Debnath, and Saha (2013), who reported the synthesis of AINPs from the tea extract. The synthesized nanoparticles were characterized by Nanoparticle Tracking Analysis (NTA) (LM20 limited, UK). This characterization was performed to determine the average size and the concentration of synthesized nanoparticles. The SNPs were found to be of 53 ± 49 nm (Fig. 2(A)) size and 3 × 10<sup>6</sup> particles/mL concentration. While the size of AINPs was 39 ± 35 nm (Fig. 2(B)) with 1.21 × 10<sup>8</sup> particles/mL concentration. NTA analysis depends on the brownian motion of the particles, and particles by particles size distribution, recorded by the instrument (Tiwari, Pandit, Gaikwad & Rai, 2017). Zeta potential was measured to assess the surface charge and the stability of mycosynthesized SNPs and AINPs, which was determined by zetasizer. The magnitude of zeta potential gives an indication of the potential stability of the colloidal system. Zeta potentials of SNPs and AINPs were recorded as +2.37 mV (Fig. 3(A)) and +1.53 mV (Fig. 3(B)) respectively.

XRD was performed to determine the crystalline nature of nanoparticles. SNPs showed its characteristic diffraction peaks at 15.6°, 23.08°, 25.94°, 31.65°, 37.22°, 42.91°, 47.18°, which depicts the presence of facets of FCC structure at (113), (220), (222), (044), (422), (319), (515) (Fig. 4(A)). These values correlate with JCPDS (Joint Committee on Powder Diffraction, Standard) file No. N34-094. The diffraction pattern of SNPs showed similarity with the results

reported by Awwad et al. (2015). The synthesized AINPs demonstrated its characteristic diffraction peak at  $38^\circ$ ,  $44^\circ$ ,  $67^\circ$  which depicts the presence of (100), (113), (214) facets of FCC structure (Fig. 4(B)). These values match with JCPDS file No. 42–1468, which corroborates with the study of Ansari et al. (2015). The morphology, size and crystalline pattern of SNPs and AINPs were determined by TEM and Selected Area Electron Diffraction (SAED). SNPs were spherical with 50 nm size (Fig. 5(A)) while AINPs were found to be 30 nm with spherical shape (Fig. 5(B)). The crystalline nature of nanoparticles was confirmed from SAED pattern, images produced by SNPs and AINPs. The appearance of dark and bright dots represent the crystalline nature of nanoparticles. The antimicrobial activity of SNPs and AINPs were tested against *C. violaceum*, *L. monocytogenes*, *S. typhi*, *Foxysporum* and *A. flavus*. It was found that SNPs and AINPs both showed significant activity against all the test microorganisms. SNPs were highly effective against *S. typhi* (Zone of inhibition was 21 mm), followed by *F. oxysporum*, *C. violaceum*, *A. flavus* and the least activity was noted against *L. monocytogenes* (Zone of inhibition was 13 mm). Suleiman et al. (2015) reported high activity of SNPs against *S. aureus* followed by *E. coli*, *P. aeruginosa* and *Aspergillus* sp. The authors also reported that SNPs are significantly effective against many Gram positive and Gram negative bacteria of agricultural and medical importance (Choudhury, Ghosh, & Goswami, 2012). Choudhury et al., (2011) reported antimicrobial activity of SNPs against food spoilage fungi *Aspergillus niger*. *A. niger* cause contamination in certain fruits, vegetables, nuts, cereals and bean. AINPs showed maximum efficacy against *F. oxysporum* and least against *L. monocytogenes*. Similarly, Geoprincy, Gandhi, and Renganathan (2012) reported antibacterial activity of AINPs against *Bacillus cereus* and *Bacillus subtilis*. Mukherjee, Sadiq, Prathna and Chandrasekaran (2011) also reported antimicrobial potential of aluminium oxide nanoparticles. The essential oils extracted from *C. medica* and *E. globulus* showed antimicrobial activity against all the pathogens tested in the present study. Nanofunctionalized oils demonstrated superior antimicrobial activity against all the pathogens tested as compared to SNPs, AINPs and EOs when tested separately. It was observed that nanofunctionalized oil containing SNPs was most effective against *S. typhi*, followed by *F. oxysporum*, *C. violaceum*, *A. flavus* whereas,

least activity was noted against *L. monocytogenes*. Nanofunctionalized oil with AINPs showed maximum activity against *F. oxysporum* and least against *L. monocytogenes* (Fig. 6(A,B,C,D)). The present study shows resemblance with the results reported by Scandorieiro et al. (2016), who found enhanced antimicrobial activity of silver nanoparticles in combination with the essential oil of

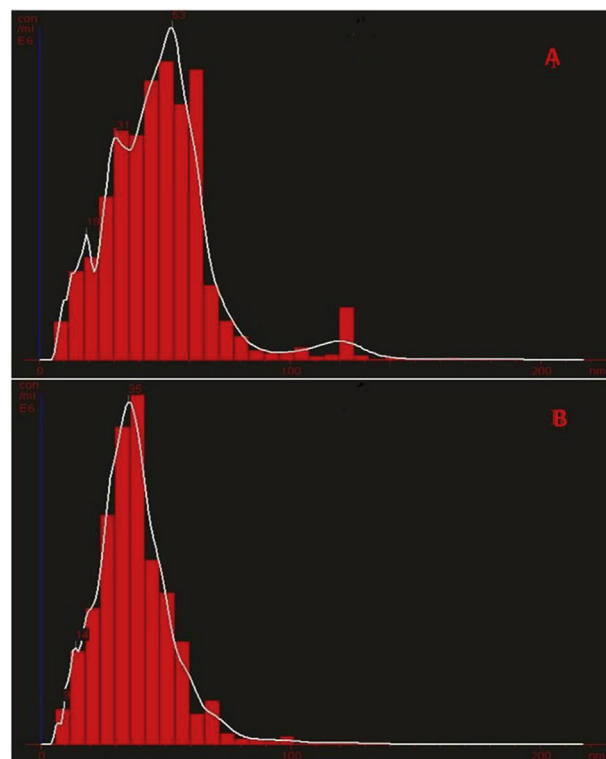


Fig. 2. Nanoparticle tracking analysis histogram showing size distribution and average size (A) Sulphur nanoparticles with average size of 53 nm (B) Aluminium oxide nanoparticles with average size of 39 nm).

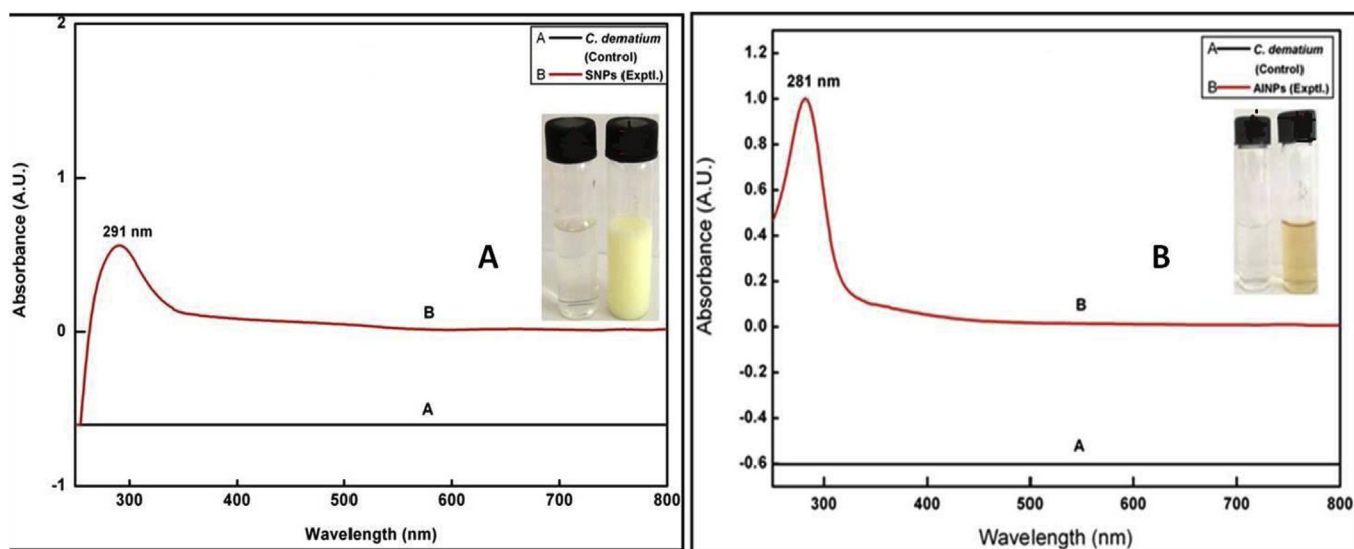
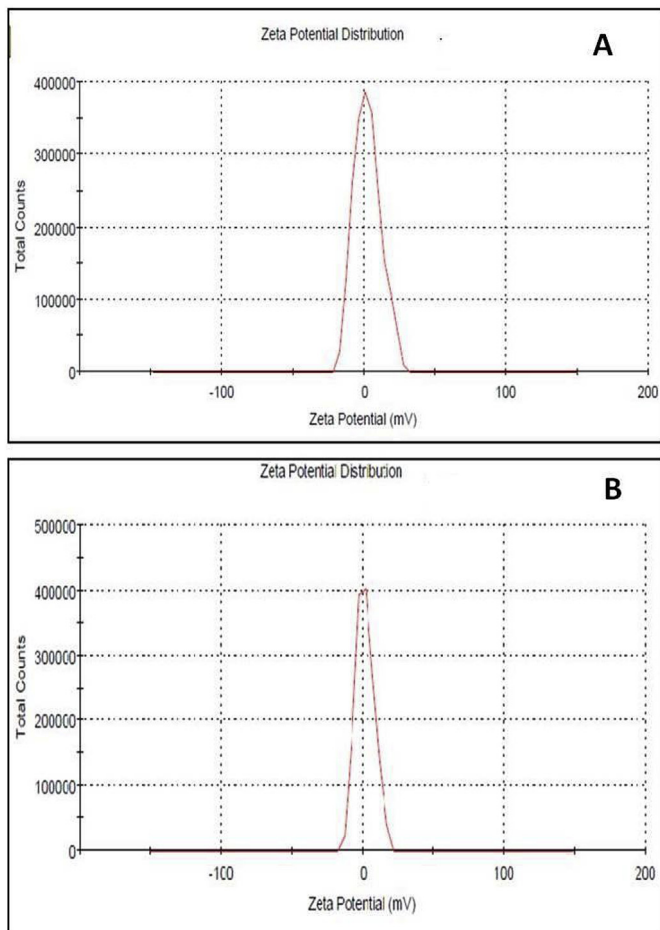
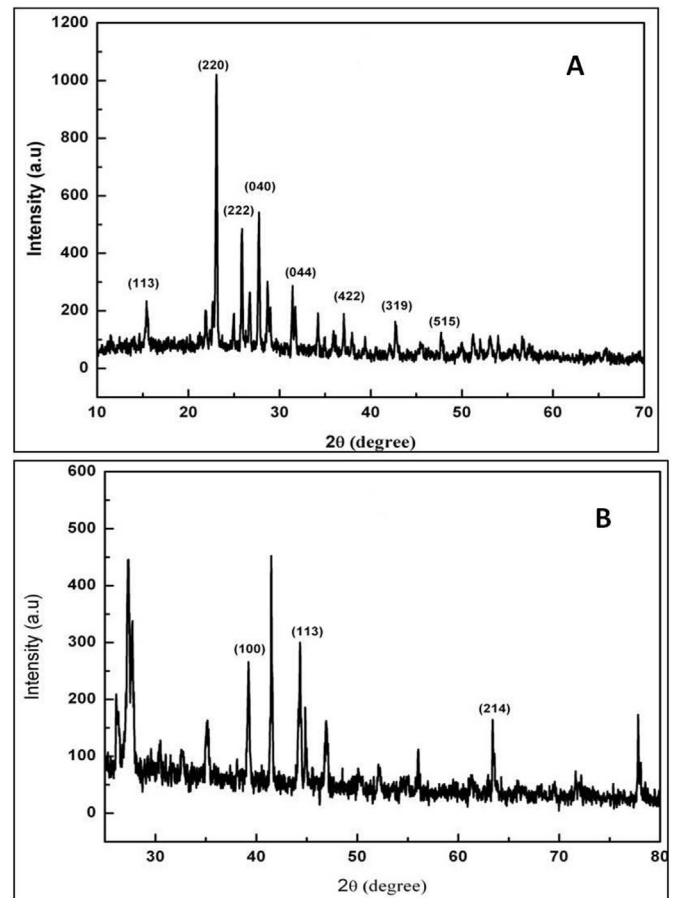


Fig. 1. UV-Vis spectra (A) Sulphur nanoparticles (inset figure shows change in colour from colourless fungal extract to yellow turbid solution on treatment of precursor) showing its characteristics absorbance at 291 nm (Spectra A- *Collectotrichum* sp. fungal extract, Spectra B- sulphur nanoparticles). (B) Aluminium oxide nanoparticles (inset figure shows change in colour from colourless fungal extract to brown solution) showing its characteristics absorbance at 281 nm (Spectra A- *Collectotrichum* sp. fungal extract, Spectra B- aluminium oxide nanoparticles). (For interpretation of the references to colour in this figure legend, the reader is referred to the web version of this article.)



**Fig. 3.** Zeta potential measurement graphs (A) Sulphur nanoparticles showing zeta potential value + 2.37 mV (B) Aluminium oxide nanoparticles showing zeta potential value + 1.53 mV.



**Fig. 4.** Powder X-ray diffraction pattern of nanoparticles (A) Sulphur nanoparticles exhibited  $2\theta$  peaks at  $15.6^\circ$ ,  $23.08^\circ$ ,  $25.94^\circ$ ,  $31.65^\circ$ ,  $37.22^\circ$ ,  $42.91^\circ$ ,  $47.18^\circ$ , which may be indexed to (113), (220), (222), (044), (422), (319), (515) facets of Face Centered Cubic structure of sulphur nanoparticles. (B) Aluminium nanoparticles exhibited peaks at  $38^\circ$ ,  $44^\circ$ ,  $67^\circ$  which may be indexed to (100), (113), (214) facets of Face Centered Cubic structure of aluminium oxide nanoparticles and indicating crystalline nature of synthesized nanoparticles.

oregano against Multi Drug Resistant (MDR) bacteria. The antimicrobial activity of SNPs and AINPs were also evaluated in combination with commercially available antibiotics such as tetracycline, oxytetracycline, gentamicin, fluconazole, ketoconazole, nystatin and amphotericin B. It was found that antibacterial activity of commercially available antibiotics was increased in presence of SNPs and AINPs against *S. typhi*, *C. violaceum* and *L. monocytogenes*. The increased in fold area for both the nanoparticles was maximum in combination with gentamicin as compared to tetracycline and oxytetracycline. The antifungal activity of SNPs in combination with amphotericin B was maximum against *A. Flavus* followed by *F. oxysporum*, when combined with ketoconazole. The antifungal activity of AINPs in combination with fluconazole was maximum against *A. niger* and *F. oxysporum* as compared to other antibiotics. Synergistic antimicrobial activity was observed when nanoparticles were combined with all the commercially available antibiotics. This study showed similarity with the results obtained by Bawaskar et al. (2010), who reported that activity of antibiotics enhances in combination with silver nanoparticles. Increase in fold area was also calculated, when EOs were combined with SNPs and AINPs. After functionalization of SNPs with citrus and eucalyptus oil, the fold area was increased to maximum against *S. typhi* followed by *L. monocytogenes*. When AINPs were functionalized with both EOs it was observed that increase in fold area was highest against *F. oxysporum* followed by *L. monocytogenes*. After determination of MIC of bacteria, TTC was added in 96- well plate. Appearance of

pink colour in the microtiter plate was due to the reduction of TTC and formation of red colour complex formazan indicate the viable active growth of bacteria. The well which did not retain colour and appear colourless, was due to the inhibition of bacterial growth and represents MIC of nanoparticles. MIC of SNPs was found to be the least for *S. typhi* (250  $\mu\text{g}/\text{mL}$ ) and maximum for *L. monocytogenes* (700  $\mu\text{g}/\text{mL}$ ). Whereas, the MIC value of AINPs was least for *F.oxysporum* (150  $\mu\text{g}/\text{mL}$ ), and maximum for *L. monocytogenes* (1000  $\mu\text{g}/\text{mL}$ ) (Table 1).

#### 4. Conclusion

The mycosynthesis of SNPs and AINPs from endophytic *Colletotrichum* sp. is simple and cost-effective. The activity of both nanoparticles showed significant antimicrobial activity against food-borne pathogens such as *Chromobacterium violaceum*, *Listeria monocytogenes*, *Salmonella typhi*, *Fusarium oxysporum* and *Aspergillus flavus*. Nanofunctionalized oil was formulated by combination of EOs (*Eucalyptus globulus* and *Citrus medica*) with SNPs and AINPs, which showed significant antimicrobial activity as compared to nanoparticles and EOs tested separately. Moreover, SNPs and AINPs demonstrated synergistic activity with commercially available antibiotics such as tetracycline, oxytetracycline, gentamicin, fluconazole, ketoconazole, amphotericin B and nystatin. Biologically

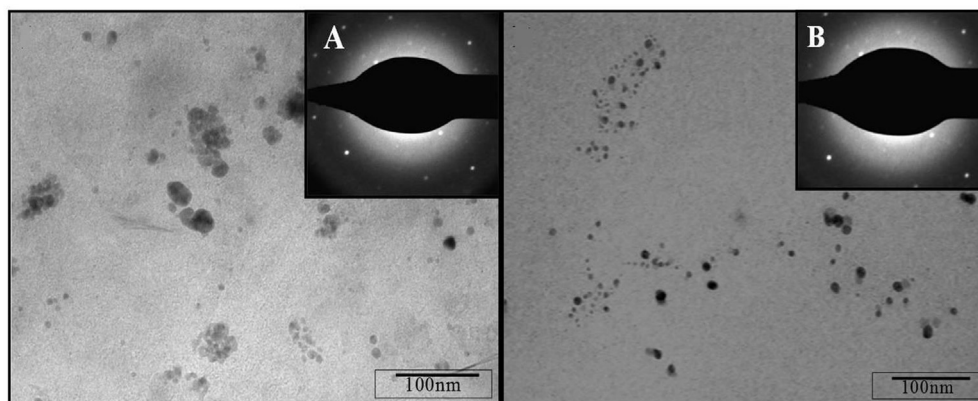


**Fig. 5.** Transmission electron micrograph (A) Sulphur nanoparticles with the size of 50 nm and inset figure of selected area electron diffraction pattern which shows bright rings depicting the Face Centered Cubic structure and indicating the crystalline nature of sulphur nanoparticles (B) Aluminium oxide nanoparticles with the size of 30 nm and selected area electron diffraction pattern in the inset showing bright rings, which reveals face centered cubic structure of aluminium oxide nanoparticles.

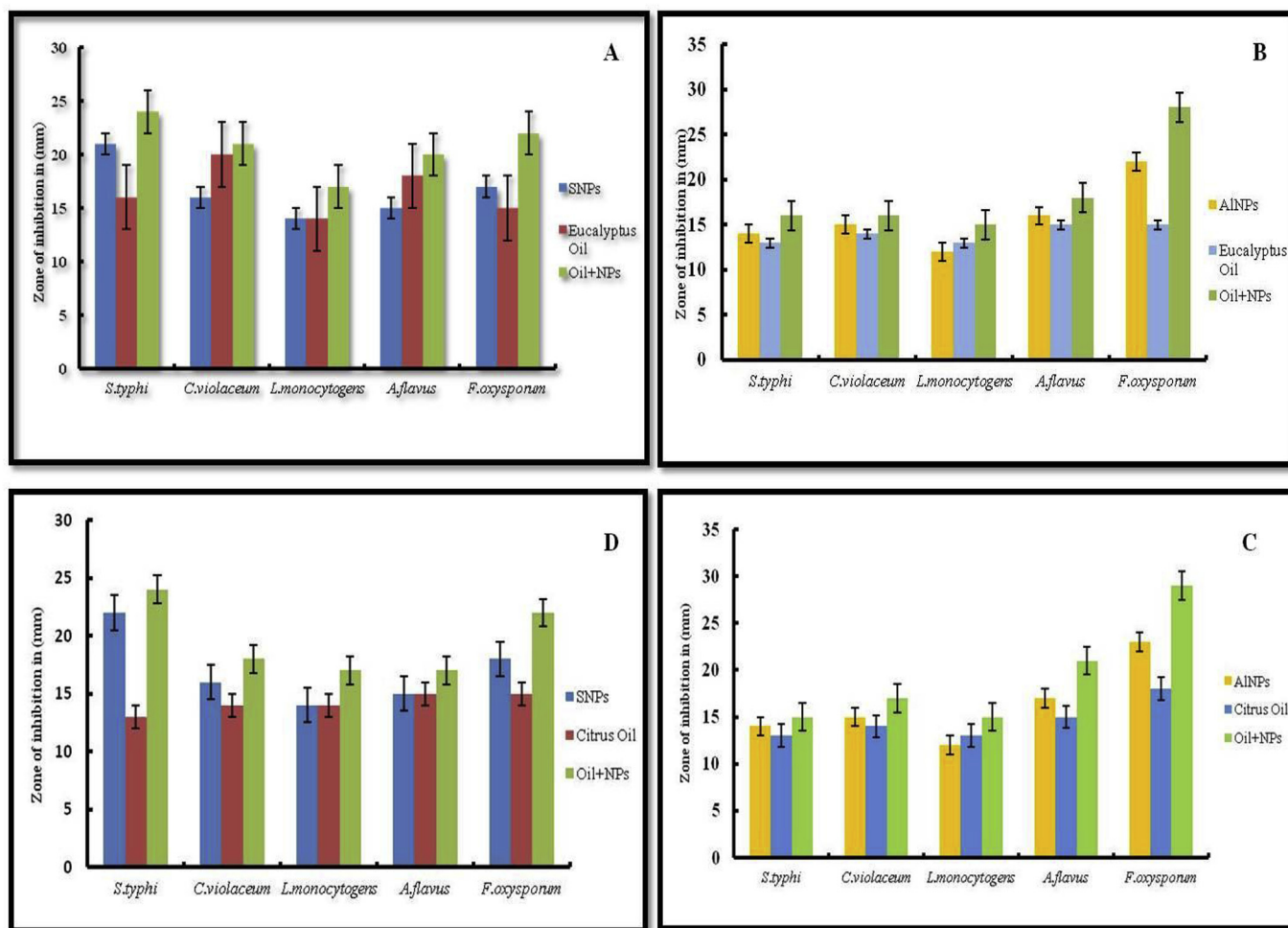


**Fig. 6.** *In vitro* antimicrobial activity of nanoparticles singly and in combination with essential oil against food borne pathogens such as *Listeria monocytogenes*, *Salmonella typhi*, *Chromobacterium violaceum*, *Fusarium oxysporum* and *Aspergillus flavus*. (A) Sulphur nanoparticles, eucalyptus oil and combination of sulphur nanoparticles with eucalyptus oil (nanofunctionalized oil) (B) *In vitro* antimicrobial activity of aluminium oxide nanoparticles, eucalyptus oil and combination of aluminium oxide nanoparticles with eucalyptus oil (nanofunctionalized oil) (C) Aluminium oxide nanoparticles, *Citrus medica* oil and combination of *Citrus medica* oil (nanofunctionalized oil) (D) Sulphur nanoparticles, *Citrus medica* oil and combination of sulphur nanoparticles with *Citrus medica*.

*In vitro* antimicrobial assay was performed in triplicate and the standard deviation is represented in the graph with the help of standard error bars.

**Table 1**  
Minimum inhibitory concentration of sulphur nanoparticles (SNPs) and aluminium oxide (AINPs) against *Salmonella typhi*, *Chromobacterium violaceum*, *Listeria monocytogenes*, *Aspergillus flavus* and *Fusarium oxysporum*.

Name of the strain	MIC in µg/mL	
	SNPs	AINPs
<i>S. typhi</i>	250 ± 1.21	400 ± 1.08
<i>C. violaceum</i>	450 ± 0.87	300 ± 2.36
<i>L.monocytogenes</i>	700 ± 1.88	1000 ± 1.1
<i>A. flavus</i>	550 ± 2.16	250 ± 0.65
<i>F. oxysporum</i>	400 ± 0.54	150 ± 2.77

The Minimum Inhibitory Concentration of Sulphur and Aluminium oxide nanoparticles was performed in triplicate. Standard deviation values are given in the above mentioned table.

synthesized SNPs and AINPs can be used as novel antimicrobial agent in combination with EOs, which will help in prevention of food-borne pathogens. In addition, it can serve as an efficient way to increase the bioavailability.

## Acknowledgment

The Authors are thankful to University Grants Commission (F3-16/2012(SAP II)), New Delhi for financial assistance under UGC-SAP Programme; to Department of Science and Technology (IF150452), New-Delhi for financial support under Indo-Argentina programme and RP acknowledges Department of Science and Technology, New Delhi, India for providing DST-INSPIRE fellowship to pursue research work. SZ and MD acknowledges ANPCyT for the grant PICT 2014-1170.

## References

Ahmed, J., Hiremath, N., & Jacob, H. (2016). Antimicrobial efficacies of essential oils/nanoparticles incorporated polylactide films against *L. monocytogenes* and *S. typhimurium* on contaminated cheese. *International Journal of Food Properties*. <http://dx.doi.org/10.1080/10942912.2015.1131165>.

Ansari, A. M., Khan, M. H., Alzohairy, M. A., Jalal, M., Ali, G. S., Pal, R., et al. (2015). Green synthesis of Al<sub>2</sub>O<sub>3</sub> nanoparticles and their bactericidal potential against clinical isolates of multi-drug resistant *Pseudomonas aeruginosa*. *World Journal of Microbiology and Biotechnology*, 31, 153–164.

Awwad, A. M., Salem, N. M., & Amany, O. (2015). Novel approach for synthesis of sulfur (s-nps) nanoparticles using *Albizia julibrissin* fruit extract. *DOI:10.5185.5792 Advance Material Letters*.

Bauer, A. W., Roberts, C. E., & Kirby, W. M. (1960). Single disc versus multiple disc and plate dilution techniques for antibiotic sensitivity testing. *Antibiotic Annual*, 7, 574–580.

Bawaskar, M., Gaikwad, S., Ingle, A., Rathod, D., Gade, A., Duran, N., et al. (2010). A new report on mycosynthesis of silver nanoparticles by *Fusarium culmorum*. *Current Nanoscience*, 6, 376–380.

Chaudhuri, R. G., & Paria, S. (2011). Growth kinetics of sulfur nanoparticles in aqueous surfactant solutions. *Journal of Colloid and Interface Science*, 354, 563–569.

Choudhury, S. R., Ghosh, M., & Goswami, A. (2012). Inhibitory effects of sulfur nanoparticles on membrane lipids of *Aspergillus Niger*: A novel route of fungistasis. *Current Microbiology*. <http://dx.doi.org/10.1007/s00284-012-0130-7> 65 91–97.

Choudhury, S. R., Ghosh, M., Mandal, A., Chakravorty, D., Pal, M., Pradhan, S., et al. (2011). Surface-modified sulfur nanoparticles: An effective antifungal agent against *Aspergillus Niger* and *Fusarium oxysporum*. *Applied Microbiology and Biotechnology*, 90, 733–743.

CLSI. (2002). *Reference method for broth dilution antifungal susceptibility testing of filamentous fungi; approved standard*. CLSI document M38-A. CLSI, Pennsylvania. ISBN 1-56238-470-8.

Faleiro, L. M. (2011). The mode of antibacterial action of essential oils in science against microbial pathogens. In A. Mendez-Vilas (Ed.), *Communicating current research and technological advances* (pp. 1143–1156). Spain: Formatex, Research Center.

Geopriancy, G., Gandhi, N., & Renganathan, S. (2012). Novel antibacterial effects of alumina nanoparticles on *Bacillus cereus* and *Bacillus subtilis* in comparison with

antibiotics. *International Journal of Pharmacy and Pharmaceutical Sciences*, 3(4), 511–544.

Hosseini, S. F., Zandi, M., Rezaei, M., & Farahmandghav, F. (2013). Two-step method for encapsulation of oregano essential oil in chitosan nanoparticles: Preparation, characterization and *in vitro* release study. *Carbohydrate Polymers*, 95, 50–56.

Hyltdgaard, M., Mygind, T., & Meyer, R. (2012). Essential oils in food preservation mode of action, synergies and interactions with food matrix components. *Frontiers in Microbiology*, 3(12), 1–24.

Käferstein, F. K., Mortarjemi, Y., & Bettcher, D. W. (1997). Food-borne disease control: A transnational challenge. *Emerging Infectious Diseases*, 3, 503–510.

Le, A. T., Huy, P. T., Tam, L. T., Tam, P. D., Hieu, N., & Huy, T. (2011). Novel silver nanoparticles: Synthesis, properties and applications. *International Journal of Nanotechnology*, 8(3), 278–290.

Mead, P. S., Slutsker, L., Dietz, V., McCaig, L. F., Bresee, J. S., Shapiro, C., et al. (1999). Food-related illness and death in the United States. *Emerging infectious diseases*, 5, 607–625.

Mith, H., Dure, R., Delcenserie, V., Zhiri, A., Daube, G., & Clinquart, A. (2014). Antimicrobial activities of commercial essential oils and their components against food-borne pathogens and food spoilage bacteria. *Food Science & Nutrition*, 2(4), 403–416.

Moghaddam, A. B., Namvar, F., Moniri, M., Paridah, T. S., & Mohamad, M. (2015). Nanoparticles biosynthesized by fungi and yeast: A review of their preparation, properties, and medical applications. *Molecules*, 20(9), 16540–16565.

Mukherjee, A., Sadiq, M., Prathna, T. C., & Chandrasekaran, N. (2011). Antimicrobial activity of aluminium oxide nanoparticles for potential clinical applications. In A. Mendez-Vilas (Ed.), *Science against microbial pathogens: Communicating current research and technological advances* (pp. 245–251). Spain: Formatex, Research Center.

Nazzaro, F., Fratianni, F., Martino, L. D., Coppola, R., & Feo, V. D. (2013). Effect of essential oils on pathogenic bacteria. *Pharmaceuticals*, 6, 1451–1474.

Pecarsaki, D., Jugovic, X. K., Brankovic, S. D., Mihajilovski, K., & Jankovic, S. (2014). Preparation, characterization and antimicrobial activity of chitosan microparticles with thyme essential oil. *Hemijiska Industrija*, 68(6), 721–729.

Rai, M., Yadav, P., Bridge, P., & Gade, A. (2009). Myconanotechnology (NT), a new and emerging science. In M. Rai, & Bridge (Eds.), *Applied mycology* (pp. 258–267). London: CAB International.

Rai, M., Yadav, A., & Gade, A. (2011). Mycofabrication, mechanistic aspect and Multifunctionality of Metal Nanoparticles - where are we? And where should we go? In A. Mendez-Vilas (Ed.), *Current research, Technology and education Topics in applied microbiology microbial Biotechnology* (pp. 1343–1354). Spain: Formatex, Research Center.

Ramos, E. H. S., Moraes, M. M., de, A., Nerys, L. L., Nascimento, S. C., Militão, G. C. G., et al. (2014). Chemical composition, leishmanicidal and cytotoxic activities of the essential oils from *Mangifera indica* L. var. Rosa and Espada. *Biomedical Research International*, 2014. <http://dx.doi.org/10.1155/2014/734946>.

Saxena, J., Sharma, M. M., Gupta, S., & Singh, A. (2014). Emerging role of fungi in nanoparticles synthesis and their applications. *World Journal of Pharmacy and Pharmaceutical Sciences*, 3, 1586–1613.

Scandorieiro, S., Larissa, C., Camargo, D., Cesar, A., Lancharos, C., Sueli, F., et al. (2016). Synergistic and additive effect of oregano essential oil and biological silver nanoparticles against multidrug-resistant bacterial strains. *doi: 10.3389.2016.00760 Frontiers in Microbiology*, 7, 760.

ShivShankar, S., Ahmad, A., Pasricha, R., & Sastry, M. (2003). Bioreduction of chloroaurate ions by geranium leaves and its endophytic fungus yields gold nanoparticles of different shapes. *Journal of Material Chemistry*, 13, 1822–1826.

Singh, R., & Singh, N. H. (2011). Medical applications of nanoparticles in biological imaging, cell labeling, antimicrobial agents, and anticancer and nanodrugs. *Journal of Biomedical Nanotechnology*, 7(4), 489–503.

Souza, M. A. A., Lemos, M. J., Brito, D. M. C., Fernandes, M. S., Castro, R. N., & Souza, S. R. (2014). Production and quality of menthol mint essential oil and antifungal and antigerminative activity. *American Journal of Plant Sciences*, 5, 3311–3318.

Suleiman, M., Masri, M. A., Ali, A. A., Aref, D., Hussein, A., Saadeddin, I., et al. (2015). Synthesis of nano-sized sulfur nanoparticles and their antibacterial activities. *Journal of Materials and Environmental Science*, 6(2), 513–518.

Sutradhar, P., Debnath, N., & Saha, M. (2013). Microwave-assisted rapid synthesis of alumina nanoparticles using tea, coffee and triphala extracts. *Advance Manufacture*, 1(4), 357–361.

Tiwari, N., Pandit, R., Gaikwad, S., & Rai, M. (2017). Biosynthesis of Zinc oxide nanoparticles by petal extract of *Rosa indica* its formulation as nail paint and evaluation of antifungal activity against fungi causing onychomycosis. *IET Nanobiotechnology*, 11, 205–211.

Wayne, P. A. (2002). *National Committee for Clinical Laboratory Standards. Reference method for broth dilution antifungal susceptibility testing of filamentous fungi. Approved standard, M27-A*.

Yadav, A., Kon, K., Kratosova, G., Duran, N., Ingle, A. P., & Rai, M. (2015). Fungi as an efficient mycosystem for the synthesis of metal. *Biotechnology Letters*, 37, 2099–2120.